# ORBIT: Optimized Routing for Bridge Inspection Toolkit. An open-source UAS flight path planning tool for comprehensive bridge inspections under realistic constraints

Erkki T. Bartczak\*1, Maarten Bassier1 and Maarten Vergauwen1

<sup>1</sup>Department of Civil Engineering, Faculty of Engineering Technology, Geomatics Research Group, KU Leuven Gebroeders De Smetstraat 1, B-9000 Gent, Belgium – erkkitobias.bartczak@kuleuven.be, maarten.bassier@kuleuven.be, maarten.vergauwen@kuleuven.be

Keywords: UAS, bridge inspection, flight path planning, infrastructure monitoring, photogrammetry

#### **Abstract**

Manual bridge inspections are labour-intensive, hazardous, and costly. While unmanned aerial system (UAS) are promising to facilitate the process, current flight planning tools do not address the unique challenges of complex bridge geometries or GNSS-denied underdeck environments. We present ORBIT, an open-source toolkit for generating optimized waypoint routes specifically designed bridge inspection missions using only minimal prior data. ORBIT generates coordinated waypoint routes for overview and underdeck inspections, maintaining spatial overlap between datasets to facilitate accurate image alignment. This approach also allows the UAS to closely follow bridge side faces at constant offsets, optimizing data acquisition for damage detection tasks. The planning workflow supports integration of commonly available cross-sectional plans or satellite imagery, incorporates flexible safety zones, and exports missions in standard KML and KMZ formats for direct use even with off-the-shelf commercial drones. Field deployments on multiple concrete canal bridges demonstrate that the generated routes provide complete inspection coverage. Underdeck missions were successfully executed using a DJI Mavic 3 Enterprise, relying solely on its onboard IMU when GNSS was unavailable and achieving reliable operation for bridge spans up to 20 meters. By making ORBIT openly available, this work aims to enable safer, more precise, and scalable UAS-based bridge inspection, and to support future research in the field. https://github.com/ErToBar2/ORBIT

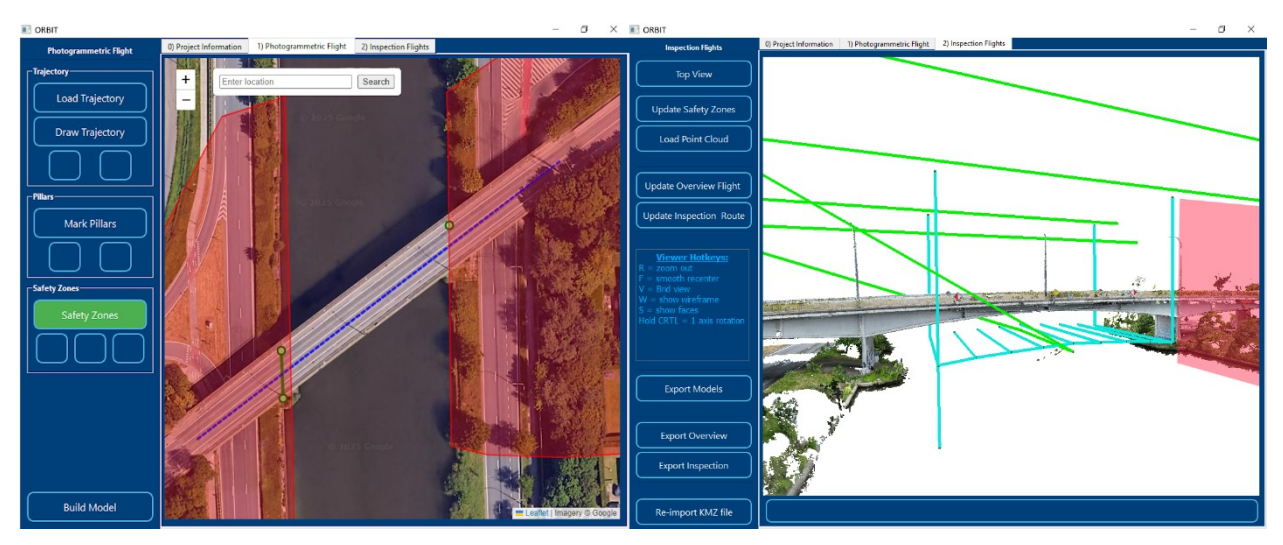


Fig. 1: Graphical User Interface (GUI) of ORBIT. The main input tab displays satellite imagery with user-defined bridge trajectories and safety zones (left), generated overview flight route in green and underdeck inspection route in blue (right).

# 1. Introduction

Bridge inspections play a crucial role in infrastructure management, ensuring that critical transportation assets remain safe, reliable, and serviceable over their operational lifetimes. Historically, inspectors have relied on labour-intensive methods, such as scaffolding or rope access, to document damage and schedule repair actions. These conventional approaches can be expensive, time-consuming, and hazardous. By contrast, UASs have the potential to capture high-resolution imagery of vulnerable areas more efficiently and with reduced risk to inspection personnel (Morgenthal et al., 2019).

Beyond visual documentation, UAS-based inspections encompass diverse tasks such as creating photogrammetric 3D models (Chen et al., 2019), automated damage detection (Kerle et al., 2020), and even structural analysis (Hamdan et al., 2021).

These downstream tasks are directly influenced by the quality of the UAS imagery. However, most studies in this area rely on manual flights (Panigati et al., 2025), which introduce human error and limit the scalability of UAS-assisted bridge inspections. In contrast, executing preplanned flight paths has the potential to improve data quality, on-site efficiency, and mission safety.

Generally, predefined flight paths can be generated using industry-standard commercial solutions such as e.g. *DroneDeploy, Pix4Dcapture* or *DJI FlightHub.* However, these tools typically focus on mapping missions that employ regular grids or linear flight paths above the object of interest. By contrast, practical flight path planning for bridge inspections requires supporting fully three-dimensional routes, accommodating GNSS-denied environments, and adhering to regulatory restrictions, i.e., line-of-sight requirements, no-fly

zones over traffic, and minimum distances from uninvolved persons. Recent research tends to focus on either fully autonomous path planning or 3D model-based flight-route computation (Wang et al., 2022; Tang et al., 2024). Unfortunately, such approaches often call for highly specialized UAS platforms or highly accurate 3D models, which may not be available.

This paper addresses these shortcomings by introducing a practical and flexible flight-planning tool specifically designed for bridge inspections under realistic constraints. Our key contributions are as follows:

- Open-source GUI: A graphical user interface that integrates satellite imagery and minimal structural data to generate flight paths for 3D mapping and bridge inspection purposes.
- Safety-oriented planning: The system incorporates safety zones for obstacles such as e.g. vegetation, power lines and traffic and consider UAS regulations.
- Semi-automated approach: Route navigation is automated, while the pilot retains camera control for maximum flexibility.
- Real-world validation: We quantify flight-path execution accuracy and test a off-the-shelf UAS under challenging GNSS-denied conditions.

By packaging these elements into a cohesive workflow, we seek to promote more efficient and safer UAS data acquisition for bridge inspections and therefore facilitate downstream research areas.

The remainder of this paper is organized as follows: Section 2 reviews relevant literature on UAS-based inspections and existing flight path generation. Section 3 details our proposed methodology for our flight route generation tool. Section 4 presents the case study, illustrating the feasibility of our approach under real-world conditions. Section 5 presents the results of the study, including metrics for flight accuracy and stability. Section 6 discusses the implications and limitations of the findings, while Section 7 concludes with a summary of contributions and recommendations for future research.

# 2. Related work

Mission-planning software for UAS based bridge inspections can be grouped into three methodological approaches, each with characteristic advantages and shortcomings. The first relies on two-dimensional, map-centric flight design. Commercial applications such as *DroneDeploy*, *Pix4Dcapture* and *DJI FlightHub* are primarily optimised for grid or linear surveys over open terrain, whereas tools like *UgCS*, *QGroundControl* and the open-source *Mission Planner* provide greater flexibility through support for full 3D waypoint planning. However, these solutions require the operator to place waypoints manually on satellite imagery, whose top-down perspective often distorts the actual geometry of bridge structures, leading to positional offsets that complicate the planning of close-range inspection flights.

The second approach eliminates manual waypoint selection by utilizing a prior geometric model. Given a BIM, triangulated mesh or point cloud, the solutions typically sample synthetic camera poses until full surface visibility is achieved and then

threads them together with a travelling-salesman solver. Representative implementations include Wu et al. (2024), which generates offset trajectories from detailed surface meshes, as well as bridge-specific planners by Bolourian and Hammad (2020), Shang and Shen (2022) and Wang et al. (2022), which can adapt camera paths to structural features such as piers and decks. A similar mesh-based coverage approach is offered in commercial photogrammetry tools like Agisoft Metashape. While these systems produce dense, geometry-conforming flight paths, they rely on the availability of an accurate 3D model and often do not consider operational limitations such as GNSS signal loss.

A third category of approaches, known as next-best-view (NBV) planning, avoids the need for a pre-existing 3-D model by incrementally selecting camera viewpoints based on live sensor input during flight (Koch et al., 2019). While this reactive strategy is conceptually appealing and well-suited to environments with limited prior knowledge, it remains computationally demanding and has so far been demonstrated primarily in simplified test environments and simulations (Dhami et al., 2023). Additionally, these solutions typically do not yet incorporate regulatory constraints (e.g. minimum distances and maximum flight speed), which further limits their current practical field deployment.

Regardless of the chosen planning approach, reliable localisation beneath bridge decks remains a fundamental challenge. A variety of external referencing methods have been explored to account for the lost GNSS signal, including fiducial markers (Wang et al., 2023), ultrasonic beacon systems (Kang and Cha, 2018), and ultra-wideband (UWB) anchor networks (Wang and Wu, 2025). Other solutions use Lidar or SLAM (Campos et al., 2021) systems. These solutions can constrain positional drift, but they require significant on-site infrastructure and are typically compatible only with modified or custom-built platforms.

In addition to navigational and safety constraints, flight planning must also account for the requirements of downstream processing tasks such as photogrammetric reconstruction (e.g. Chen et al., 2019) and automated damage detection (Li et al., 2023). Structure-from-motion (SfM) pipelines, which are widely used to generate dense 3D models from image data, require substantial visual overlap and parallax between consecutive frames to reliably estimate relative camera poses. Without GNSS based geotagging, image alignment depends entirely on feature matching, making it essential to maintain continuity between underdeck and superstructure image sets. As a result, flight paths must be designed to ensure sufficient visual connectivity across all structural elements. Moreover, bridges commonly feature complex I-girder cross sections, whose vertical and horizontal faces cannot be adequately captured from upwards nadir views alone. Planning algorithms must therefore accommodate multi-directional viewpoints that provide adequate coverage of these occluded surfaces while preserving the geometric conditions needed for successful reconstruction. Regarding the flight route requirements for damage detection, image acquisition should ideally follow the critical structural elements such as e.g. side facades in an orthogonal perspective at close range, typically within 2-3 meters depending on sensor resolution and target defect size. This necessitates fine-grained control over both the spatial trajectory and flight speed to ensure sufficient image detail and motion blur avoidance.

Despite recent progress, significant knowledge gaps persist in the domain of UAS-based bridge inspection flight planning. There is a lack of systematic solutions for generating underdeck waypoint routes that can be reliably executed with off-the-shelf UAS, particularly in GNSS-denied environments. Proposed solutions depend either on specialized UAS hardware or the availability of detailed 3D bridge models, limiting their practicality and widespread adoption. Furthermore, existing tools rarely address safety-critical obstacles or consider the requirements of downstream tasks such as photogrammetric reconstruction and automated damage detection.

#### 3. Methodology

The proposed flight planning methodology addresses the systematic challenge of comprehensive UAS bridge inspections through a two-staged approach that effectively manages GNSS signal availability constraints, as depicted in Fig. 2. The framework consists of an initial GNSS-supported (i) overview flight for establishing reliable coordinate frameworks, followed by detailed GNSS-denied (ii) inspection flights optimized for structural coverage. This dual-stage strategy ensures robust georeferencing while enabling complete coverage, including critical underdeck regions where satellite navigation is unavailable.

The system is primarily based on the 3D trajectory of the bridge, which is commonly known to stakeholders and allows importing diverse, commonly available data sources in various formats. When existing trajectory data is available, coordinates can be imported from sources such as Excel spreadsheets or general text files. When reliable 3D trajectory data or detailed bridge models are unavailable, the system supports interactive trajectory definition through a *Leaflet*-based web mapping interface, enabling rapid mission planning with only satellite imagery and basic bridge location information.

In addition to the trajectory, the system requires a simple 2D cross-sectional profile of the bridge to generate a coarse 3D representation of its geometry. This serves primarily to compute minimal offsets from the trajectory and support the user's situational awareness during mission planning by offering a visual approximation of the bridge geometry. Crosssection drawings are typically available to infrastructure stakeholders and often follow standardized formats. The system extracts the structural shape from such drawings using OpenCV, based on a minimal input requirement: the cross section must be (manually) filled in blue, and a known measurement marked in green. Through colour-based filtering and contour detection, the profile is segmented and scaled to metric dimensions using the reference line. This 2D profile is then extruded along the predefined trajectory, producing a simple 3D volume that approximates the bridge's structure. While not intended for detailed modelling, this representation is sufficient to inform safe waypoint placement and identify critical clearances for underdeck inspection planning.

To handle varying input coordinate formats flexibly, the system leverages the Python library *PyProj*, facilitating accurate transformations into a unified local metric coordinate framework. Converting trajectory coordinates into local metric references simplifies the specification of waypoint offsets and ensures precise calculation of flight routes, inspection flight patterns, and safety clearances that closely align with the specific bridge geometry.

The overview flight establishes the global spatial reference needed to integrate inspection data acquired in GNSS-denied environments. It consists of a customizable sequence of flight segments that follow the bridge trajectory at user-defined horizontal and vertical offsets and flight speed, allowing

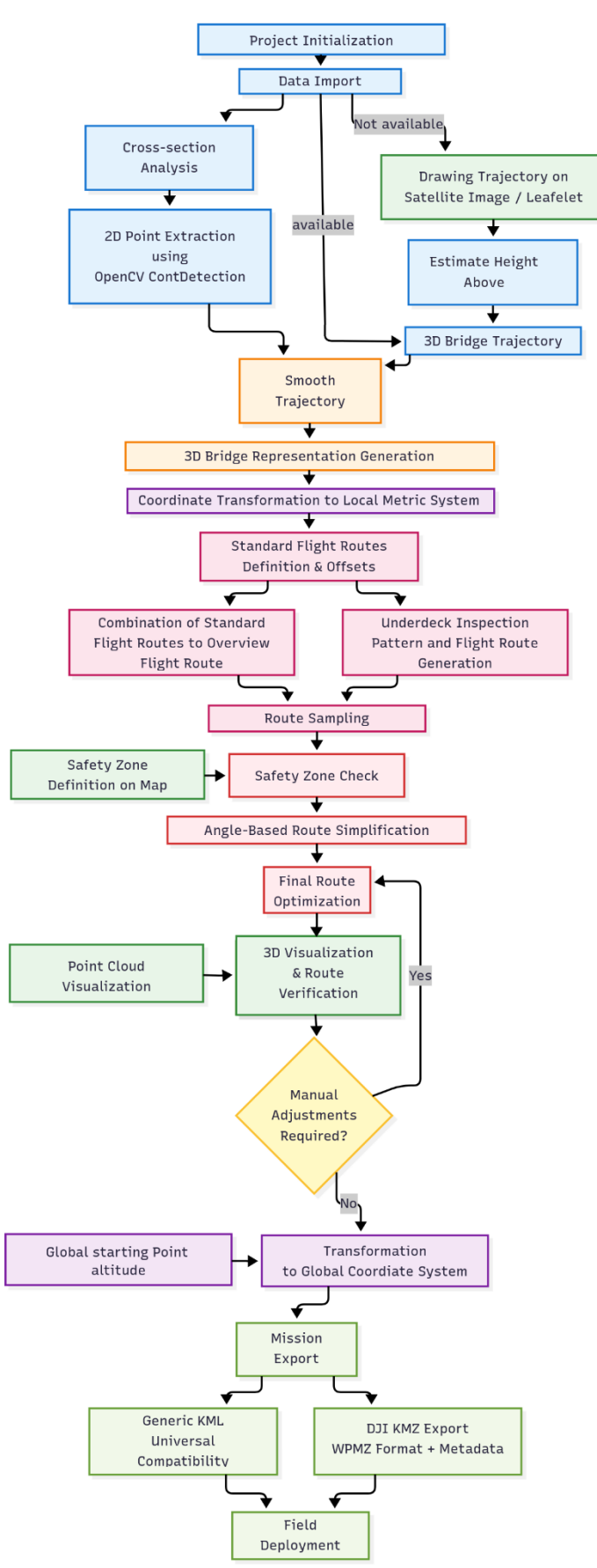


Fig. 2: ORBIT methodology flowchart. Colored blocks represent key process categories: user input (blue), satellite imagery via Leaflet (dark green), geometric representation (orange), coordinate transformations (purple), flight route generation (yellow), safety management (red), and export/deployment (light green).

operators to tailor the flight pattern to specific site conditions or structural features (Fig. 3). When the bridge trajectory is well defined, this consistently parallel flight path enables highly precise planning of follow-up façade inspections. The overview flight provides the RTK-supported imagery and is sufficient to compute an initial geolocated photogrammetric point cloud. By maintaining GNSS connectivity throughout, this phase ensures that later GNSS-denied imagery can be accurately aligned.

The underdeck inspection flight routes are designed to operate in signal-denied environments while maximizing structural coverage and positional accuracy. The system divides the bridge into spans based on user-provided pillar locations and generates systematic inspection patterns within each span. Modern UAS platforms can typically navigate short distances without GNSS by relying solely on their onboard inertial measurement units (IMU), particularly accelerometers and gyroscopes. However, these internal sensors are known to accumulate drift quickly, limiting the reliability of purely inertial navigation. To mitigate this, the inspection routes are designed to briefly exit the bridge envelope after each underdeck pass. By extending slightly beyond the span, the UAS can reacquire a stable RTK GNSS signal in open-sky conditions. This reacquisition allows the UAS to correct its position before initiating the next pass through. The periodic re-synchronization with GNSS ensures that accumulated IMU drift is minimized.

To ensure successful camera alignment during photogrammetric processing, the underdeck flights include vertical segments at the beginning and end of each inspection sequence (**Fig. 3**). These transitions guide the UAS to ascend to the same altitude as the overview flight, allowing it to capture visually consistent and overlapping imagery with the georeferenced overview dataset. This overlap enables robust camera pose estimation and effectively anchors the GNSS-denied image sets within the established global coordinate framework.

Key planning parameters such as minimum pillar clearance, lateral offset distances for GNSS signal reacquisition, and approach angles relative to the bridge alignment are fully configurable, allowing the system to adapt to a wide variety of bridge geometries and environmental constraints, including vegetation or irregular structural features.

An optional axial inspection mode is also available, generating longitudinal zigzag routes along the bridge girders. While this method offers detailed coverage, testing with standard commercial drones has shown that prolonged GNSS-denied flight results in significant navigation errors. As a result, this

mode is recommended only for advanced UAS configurations equipped with additional localization technologies such as ultra-wideband, LiDAR, or visual marker systems.

Safety zones form an integral part of the proposed risk mitigation strategy for waypoint missions, particularly when onboard obstacle avoidance systems are unavailable or inactive. While many modern UAS platforms include such features, they are often limited or disabled during preprogrammed missions. To address this limitation, the system performs a post-processing safety check after the raw flight routes have been generated. Each flight path is sampled at 1 mm intervals beforehand to support precise spatial analysis and potential remapping. Users can define polygonal 3D safety zones with customizable lower and upper altitude limits. Within these defined zones, all included waypoints are adjusted vertically to enforce specified clearance requirements from the planned flight path using a convex hull. This flexible system allows, for example, the enforcement of minimum altitudes over nearby vegetation. In scenarios where the bridge deck is regularly occupied by uninvolved persons or traffic, direct overflight may conflict with regulatory guidelines such as those defined by European Union Aviation Safety Agency (EASA). To address this, the system includes an option for underdeck transitions, allowing the drone to switch sides beneath the bridge during the overview flight without violating line-ofsight or overflight rules. Additionally, to comply with proximity regulations, flight segments that pass within 5 m of uninvolved persons can be configured to limit speed to 3 m/s, supporting safer operation in sensitive areas. Additionally, the visualization of geolocated point clouds inside the planning interface enhances situational awareness, allowing users to manually identify potential obstructions near the planned flight path and refine routes accordingly.

Flight mission export is designed for compatibility with widely used UAS platforms and common geospatial data formats. Missions are saved as KMZ files using DJI's WPMZ specification, including metadata such as drone type, payload, and mission parameters. Generic KML and simplified waypoint exports are also available to support non-DJI or custom flight controllers. Coordinate transformations are handled automatically, ensuring consistent integration regardless of the original input format. Manual camera control is preserved during flight, allowing real-time gimbal adjustments while maintaining automated navigation safety.

The Flight path deviations were assessed by comparing the camera positions ( $c_i$ ) from Structure-from-Motion (SfM) to the planned route. We resampled the planned flight path at 1 mm

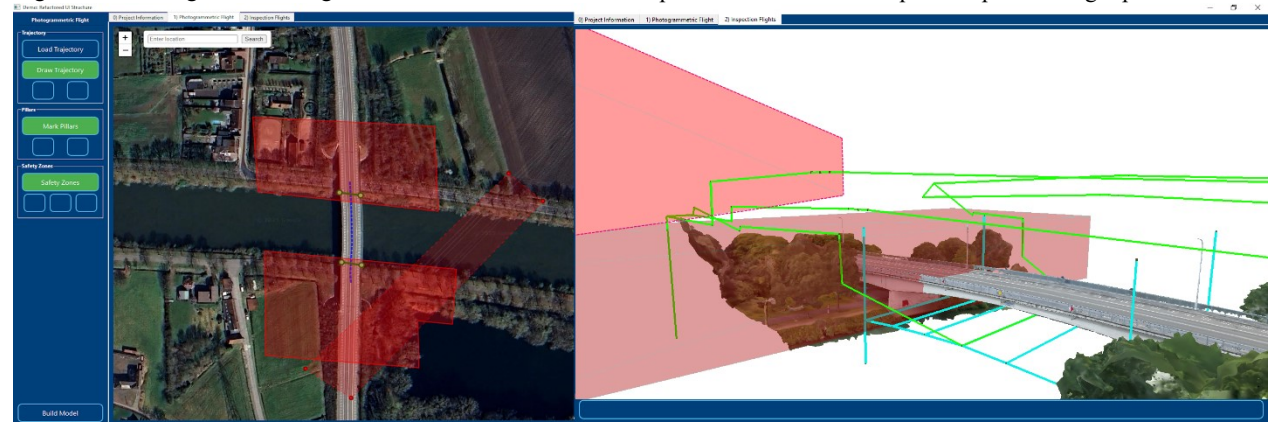


**Fig. 3: ORBIT case study demonstrating the safety zone feature.** Safety zones are defined directly on satellite imagery (left). The overview flight route (green) automatically adapts to avoid these zones. Underdeck inspection routes (blue) include vertical connections to ensure visual overlap with the overview imagery.

intervals  $(\boldsymbol{p}_j)$  and, for each camera, computed the minimum Euclidean distance  $(\boldsymbol{d}_i)$  to the path:

$$\boldsymbol{d}_i = \min_i || \boldsymbol{c}_i - \boldsymbol{p}_j ||_2$$

Horizontal and vertical components were then separated as  $\Delta XY_i = \sqrt{\Delta x_i^2 + \Delta y_i^2}$  and  $\Delta Z_i = |\Delta z_i|$ . This treats the SfM camera positions as truth. Although absolute SfM georeferencing is imperfect, earlier research showed a 3.2 cm mean distance error between the dense point cloud and terrestrial laser scans, indirectly lending support to the positions' fidelity for error analysis.

For each bridge we summarised the resulting deviations with five scalar statistics: the mean ( $\mu$ ), standard deviation ( $\sigma$ ), 95th percentile  $Q_{95\%}$ , maxima ( $\Delta XY_{max}/\Delta Z_{max}$ ), and the 3D root-mean-square error  $RMSE_{XYZ}$ .

## 4. Case study

The developed flight planning tool was employed throughout 2024 and 2025 for generating efficient and safe UAS flight paths to support bridge inspection and mapping tasks as shown in **Table 1**.

For these missions, detailed prior 3D models were not available. However, cross-sectional plans were typically provided by bridge maintainers, along with levelling data referenced to the official Belgian orthometric height system. When available, these datasets allowed immediate generation of flight paths. In cases lacking bridge trajectory data, the integrated *Leaflet*-based mapping interface was employed, and local height estimates were added, allowing for rapid trajectory definition as a fallback option.

Overview flights were systematically designed using combinations of standard flight patterns, strategically planned at multiple altitudes and distances from the bridge. Typically, a higher-level pass was executed first to provide broad coverage, followed by a closer and lower-level route to capture angled perspectives beneficial for photogrammetric reconstruction. Despite intentionally conservative offsets (approximately 10 meters horizontally and vertically) due to potential inaccuracies in height transformations using the EGM96 geoid model, the generated overview flight routes consistently resulted in high coverage. The overview flights were executed with manual camera control to ensure angled

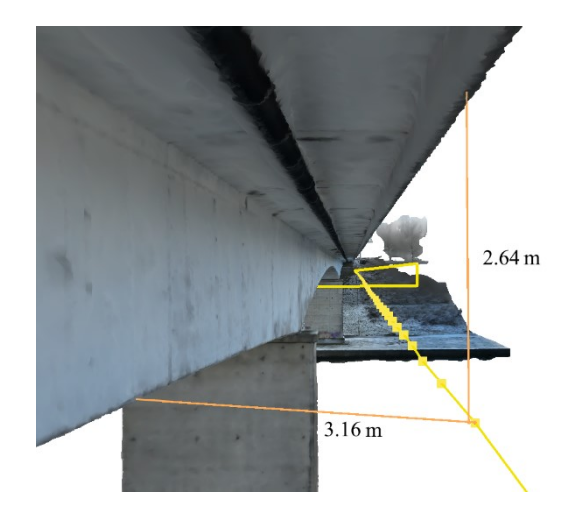


**Fig. 4.** Close-up flight route generated for detailed façade inspection.

perspectives to improve photogrammetric quality. These flights typically lasted around 10 minutes and provided RTK geolocated imagery for computing sparse point clouds on-site using *Agisoft Metashape*.

Underdeck flight routes were visually confirmed using these overview point clouds, enabling on-site verification and minor adjustments to the initial rough 3D geometry. Slight adjustments to underdeck routes were made based on the local context, using the overview point cloud to visually confirm alignment and safety. The starting point of the flight route was selected directly within the interface based on the geolocated point cloud, which enabled accurate transformation of the planned flight into the global coordinate system without relying solely on geoid-based height estimates. The underdeck inspection strategy typically involved 5–9 passes per bridge, maintaining pillar clearances of approximately 7–10 meters, and extending routes about 7 meters beyond the structure to reacquire GNSS signals.

Although a notable flight stability drift was observable due to inertial navigation under GNSS-denied conditions, most flights remained controllable and safe. However, in several cases the UAS exited the flight mission due to extended GNSS signal loss while flying under the bridge. Depending on the situation, the mission could often be resumed either directly from beneath the bridge, or alternatively by manually continuing the flight out of the underdeck area and resuming the route from the next

Table 1: Bridge information for flight planning case study

Bridge	Coordinates	Length	Width	Clearance	Note	
Bierstalbrug	51.092, 3.637	130	18.5	9.5	Successful	
Landegembrug	51.057, 3.568	120	13.5	8.5	Successful	
Nevelbrug	51.036, 3.553	125	20	9.5	Restart but successful	
Gellik-Kompveld	50.878, 5.609	175	12.5	17	Change battery, successful	
Schipdonkbrug	51.092, 3.564	120	17	9.5	Successful	
Lovendegembrug	51.091, 3.603	130	18.5	10	Successful	
Durmenbrug	51.095, 3.573	145	17.5	10	Successful	
Bellembrug	51.098, 3.495	135	18	8	Restart but successful	
Leopoldbrug	51.126, 3.375	125	18	9.5	Restart but successful	
Beekstraat	51.071, 3.658	125	13	10	Successful	
Hutsebrug	51.017, 3.709	120	36	6	Failed	
Buchtenbrug	51.034, 3.687	110	22	7	Failed	
Zwijnaarde R4	51.010, 3.735	180	18.5	9	Successful	
Zwijnaarde_A10	51.009, 3.734	145	50	6.5	Failed	

**Table 2**: Flight accuracy results

Flight route	μ <sub>ΧΥ</sub> (m)	μ <sub>Z</sub> (m)	σ <sub>χγ</sub> (m)	$\sigma_Z$ (m)	$Q_{XY_{95\%}}$ (m)	$Q_{Z_{95\%}} \  ext{(m)}$	$\Delta XY_{max}$ (m)	$\Delta Z_{max}$ (m)	$RMSE_{XYZ}$ (m)
Overview	0.13	0.33	0.10	0.14	0.33	0.51	0.59	0.6	0.44
Under- deck	0.33	0.30	0.32	0.31	0.99	0.91	1.84	1.56	0.66

All values are absolute deviations between planned and executed camera positions derived from SfM.

waypoint. While most underdeck flights were successfully completed on bridges with widths of around 18–20 meters, we observed failed missions on bridges with widths between 22 and 50 meters, particularly when combined with low vertical clearances of 5 to 7 meters. Additionally, it was observed that a clearance of at least 3 meters above water surfaces was necessary to prevent the UAS's visual positioning sensors from misinterpreting flowing water as solid ground.

In addition to the mentioned flights, for selected bridges detailed flights were successfully conducted at very close proximities (approximately 2-3 meters) to bridge sides, benefiting from precise geolocation provided by the overview point cloud. These missions delivered high resolution, orthogonal imagery which are ideal for damage detection tasks (Fig. 4).

Safety considerations were explicitly managed using configurable safety zones within the tool, typically setting vertical clearances at around 20 meters for common hazards such as trees. One notable scenario involved generating safe flight paths navigating above trees but underneath a power line at around 25 meters altitude, demonstrating the practical effectiveness of the tool's safety management capability (Fig. 3). Operational flexibility was further validated during flight interruptions due to passing ship traffic and battery replacements, with flights consistently resumed successfully. Lastly, local wind conditions were recognized as contributing significantly to positional drift during underdeck inspections, with observed drift peaks during wind gusts reaching approximately 10 m/s during our case studies.

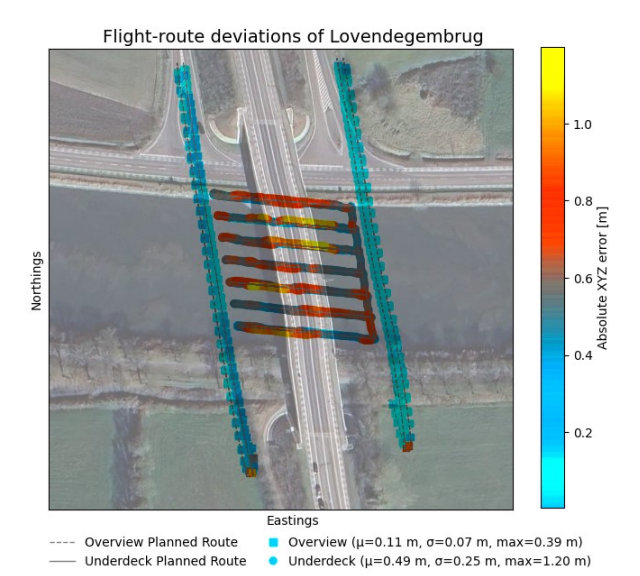


Fig. 5: Color coded absolute deviations. Planned path (grey) and executed camera positions for the case study Lovendegembrug. The lower errors are found at the overview flight (light blue), while larger deviations are observed during the underdeck passes (orange - yellow).

#### 5. Results

We analysed eight of the eleven successful missions to assess the navigation accuracy achieved under operational constraints, as summarised in **Table 2**.

All overview flights planned with the ORBIT toolkit were successfully executed across the tested set of canal bridges, producing RTK-geolocated imagery and point clouds suitable for immediate assessment and further inspection planning. These overview missions consistently achieved the intended coverage and spatial accuracy, typically requiring minimal onsite adjustment. On average, the absolute horizontal deviation was 0.13 m ( $\sigma=0.10\,\text{m}$ ), with 0.33 m ( $\sigma=0.14\,\text{m}$ ) in the vertical axis. No overview flight exceeded 0.60 m in either direction, and 95 % of points remained within a 0.33 m  $\times$  0.51 m envelope.

For the underdeck inspection flights, successful execution was strongly linked to bridge geometry, particularly span width and clearance. The underdeck inspection missions showed larger, yet consistently bounded, deviations. The mean absolute error reached  $\mu_{XY}=0.33$  m horizontally and  $\mu_Z=0.30$  m vertically, with similar scatter in both axes  $(\sigma\approx 0.32$  m). Despite repeated GNSS outages during the passes, 95 % of camera positions remained within a 1 m distance. Peak deviations reached 1.84 m (XY) and 1.56 m (Z), typically near the ends of longer IMU-only segments and during the last passes.

**Fig. 5** visually confirms the numerical findings. The overview flight stays close to its planned path, while the underdeck passes exhibit larger drifts. Error magnitudes are reduced at each turning point, indicating that the RTK signal is reacquired and the UAS updates its position before starting the next pass.

Downstream tasks such as photogrammetric reconstruction (Fig. 7) and automated damage detection (Fig. 6) were successfully performed with the collected imagery for all missions where sufficient coverage was achieved. However, these results are only briefly highlighted here, as the primary focus of this study is on the planning and execution of the inspection flights themselves.

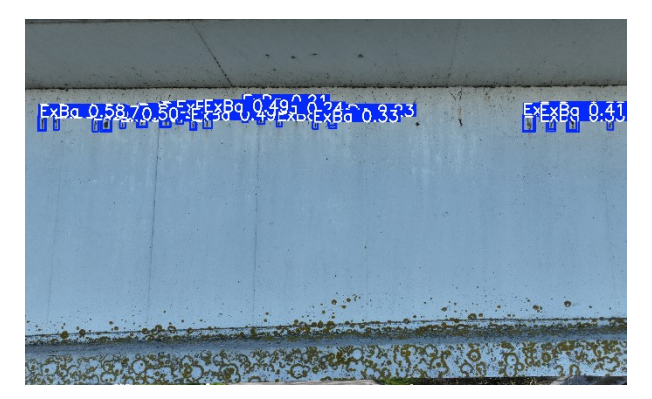


**Fig. 6:** Outcome of the façade inspection flight with automated damage detection of exposed rebars.

to-reach areas, supporting downstream tasks such as inspection and photogrammetric modelling.

Beyond the open-source toolkit, a key contribution of this work is the demonstration that off-the-shelf UAS can reliably perform semi-autonomous under-deck inspection flights by temporarily relying solely on their onboard IMU. For the deployed DJI Mavic 3 Enterprise, bridges up to approximately 20 m in width and 8 m in clearance were surveyed with mean absolute errors below 0.4 m and peak deviations generally constrained to under 2 m. These results set a practical operational envelope for commercial GNSS-reliant platforms in confined environments, without the need for prior 3D models or external navigation systems. In contrast, bridges that exceeded these geometry thresholds consistently saw increased drift or failed missions, highlighting the need for more advanced localization strategies.

To assess the consistency of navigation accuracy across individual bridges, we computed the overall root-mean-square error for each flight. Values ranged from 0.34 m at Langenburg (width = 13.5 m) to 1.28 m at Bellembrug, where the same mission recorded the largest single-point horizontal deviation,  $\Delta XY_{max} = 4.36$  m. All other underdeck flights remained below an  $RMSE_{XYZ}$  of 2.7 m. Overview flights clustered around a mean  $RMSE_{XYZ}$  of **0.44 m**, but the spread was dominated by one high-value outlier (Leopoldbrug,  $1.17\ m$ ). Excluding that case, the remaining missions ranged from 0.13 m to 0.69 m with a tighter standard deviation of 0.21 m. No systematic link emerged between  $RMSE_{XYZ}$  and bridge width or clearance, which suggests that environmental influences such as wind, local GNSS, or IMU drift contributed more to the observed variability than the static geometric parameters of the structures alone. These factors will be examined in future work.

Importantly, the results did not show a consistent dominance of error in any particular axis. Navigation drift accumulated evenly in horizontal and vertical directions, resulting in a near-symmetric 3D error distribution. In most cases, 95 % of recorded positions during under-deck flight segments remained within a 1 m radius cylinder from their planned location. This finding supports the feasibility of IMU-only segments for inspection and image alignment, provided that critical structures maintain at least a 1 m clearance from the expected trajectory.

Compared to other commercial flight planning platforms, ORBIT is built for the specific requirements of bridge inspection and reconstruction. The tool enables the generation of three-dimensional flight paths that include vertical connections between overview and underdeck segments, supporting accurate image alignment and comprehensive structural coverage. Maintaining a consistent and close proximity to the bridge surfaces facilitates thorough inspection of areas that are often difficult to access with standard grid or linear waypoint approaches e.g. for bridge façade inspections. As a result, ORBIT supports data acquisition suitable for both photogrammetric modelling and automated damage detection in bridge inspection scenarios. Finally, while the present study focused on typical 2 lane concrete canal bridges, generalizability to other bridge types (e.g., cable-stayed, arch, or multi-level structures) will require further tool development. Broader field validation across a wider range of structural types and site conditions remains an important goal for future research. Beyond bridge inspections, the tool is well suited for generating flight paths for other types of linear infrastructure, including powerline and pipeline inspections.



Fig. 7: Highly detailed photogrammetric model with high coverage in difficult to reach areas

#### 7. Conclusion

This study presented and validated the ORBIT flight planning toolkit, an open-source solution developed for practical UAS-based bridge inspection using minimal prior information. Field trials across multiple canal bridges demonstrated that semi-autonomous underdeck inspection flights are feasible with standard commercial drones for spans up to 20 meters, with results clarifying both the capabilities and current limitations of IMU-only navigation in GNSS-denied environments. Integrating the range sensors already present on many UAVs, such as upward-facing stereo vision, lidar, or radar units, into the IMU solution would allow the UAS to maintain a fixed distance to the superstructure and could further cut drift during GNSS denied underdeck inspections and widen the safe operating range for bridge inspection flights.

In summary, ORBIT's bridge-specific, three-dimensional planning approach facilitates comprehensive data acquisition for both photogrammetric reconstruction and detailed structural inspection. By making this toolkit openly available, the work aims to support continued progress in UAS-based bridge inspection research and to provide a foundation for further methodological development and broader field validation.

**Author Contributions:** E.T.B. is the main author of the work and conceived the method. M.B. is the direct supervisor. M.V. is the supervisor. All authors have read and agreed to the published version of the manuscript.

Conflicts of Interest: There are no conflicts of interest

## References

Agisoft LLC, 2022. Agisoft Metashape Professional, Version 2.0. Agisoft LLC, St Petersburg. https://www.agisoft.com (30 June 2025).

Bolourian, N., Hammad, A., 2020. LiDAR-equipped UAV path planning considering potential locations of defects for bridge inspection. *Automation in Construction* 117, 103250. DOI: 10.1016/j.autcon.2020.103250.

Campos, C., Elvira, R., Rodriguez, J.J.G., M. Montiel, J.M., D. Tardos, J., 2021. ORB-SLAM3: An Accurate Open-Source Library for Visual, Visual–Inertial, and Multimap SLAM. *IEEE Transactions on Robotics* 37 (6), 1874–1890. DOI: 10.1109/TRO.2021.3075644.

Chen, S., Laefer, D.F., Mangina, E., Zolanvari, S.M.I., Byrne, J., 2019. UAV Bridge Inspection through Evaluated 3D

Reconstructions. *Journal of Bridge Engineering* 24 (4). DOI: 10.1061/(ASCE)BE.1943-5592.0001343.

Dhami, H., Yu, K., Williams, T., Vajipey, V., Tokekar, P., 2023. GATSBI: An Online GTSP-Based Algorithm for Targeted Surface Bridge Inspection. *2023 International Conference on Unmanned Aircraft Systems (ICUAS). IEEE*, pp. 1199–1206. DOI: 10.1109/ICUAS57906.2023.10156013 DJI, 2025. FlightHub 2. DJI Enterprise. https://enterprise.dji.com/flighthub-2 (30 June 2025).

DroneDeploy, 2024. DroneDeploy. DroneDeploy Inc. https://www.dronedeploy.com (30 June 2025).

Hamdan, A.-H., Taraben, J., Helmrich, M., Mansperger, T., Morgenthal, G., Scherer, R.J., 2021. A semantic modeling approach for the automated detection and interpretation of structural damage. *Automation in Construction* 128, 103739. DOI: 10.1016/j.autcon.2021.103739.

Kang, D., Cha, Y.-J., 2018. Autonomous UAVs for Structural Health Monitoring Using Deep Learning and an Ultrasonic Beacon System with Geo-Tagging. *Computer-Aided Civil and Infrastructure Engineering* 33 (10), 885–902. DOI: 10.1111/mice.12375.

Kerle, N., Nex, F., Gerke, M., Duarte, D., Vetrivel, A., 2020. UAV-Based Structural Damage Mapping: A Review. *ISPRS International Journal of Geo-Information* 9 (1), 14. DOI: 10.3390/ijgi9010014.

Koch, T., Körner, M., Fraundorfer, F., 2019. Automatic and Semantically-Aware 3D UAV Flight Planning for Image-Based 3D Reconstruction. *Remote Sensing* 11 (13), 1550. DOI: 10.3390/rs11131550.

Li, R., Yu, J., Li, F., Yang, R., Wang, Y., Peng, Z., 2023. Automatic bridge crack detection using Unmanned aerial vehicle and Faster R-CNN. *Construction and Building Materials* 362, 129659. DOI: 10.1016/j.conbuildmat.2022.129659.

Mission Planner Development Team, 2025. Mission Planner. ArduPilot. https://ardupilot.org/planner (30 June 2025).

Morgenthal, G., Hallermann, N., Kersten, J., Taraben, J., Debus, P., Helmrich, M., Rodehorst, V., 2019. Framework for automated UAS-based structural condition assessment of bridges. *Automation in Construction* 97, 77–95. DOI: 10.1016/j.autcon.2018.10.006.

Panigati, T., Zini, M., Striccoli, D., Giordano, P.F., Tonelli, D., Limongelli, M.P., Zonta, D., 2025. Drone-based bridge inspections: Current practices and future directions.

\*Automation in Construction 173, 106101. DOI: 10.1016/j.autcon.2025.106101.

Pix4D SA, 2025. Pix4Dcapture. Pix4D SA. https://www.pix4d.com/product/pix4dcapture (30 June 2025).

QGroundControl Development Team, 2025. QGroundControl. Dronecode Foundation. https://qgroundcontrol.com/ (30 June 2025).

Shang, Z., Shen, Z., 2022. Flight Planning for Survey-Grade 3D Reconstruction of Truss Bridges. *Remote Sensing* 14 (13), 3200. DOI: 10.3390/rs14133200.

Tang, Z., Peng, Y., Li, J., Li, Z., 2024. UAV 3D Modelling and Application Based on Railroad Bridge Inspection. Buildings 14 (1), 26. DOI: 10.3390/buildings14010026.

SPH Engineering, 2025. UgCS. SPH Engineering. https://www.sphengineering.com/flight-planning/ugcs June 2025). (30

Wang, F., Zou, Y., Del Rey Castillo, E., Ding, Y., Xu, Z., Zhao, H., Lim, J.B., 2022. Automated UAV path-planning for high-quality photogrammetric 3D bridge reconstruction. *Structure and Infrastructure Engineering*. DOI: 10.1080/15732479.2022.2152840.

Wang, F., Zou, Y., Zhang, C., Buzzatto, J., Liarokapis, M., Del Rey Castillo, E., Lim, J.B., 2023. UAV navigation in large-scale GPS-denied bridge environments using fiducial marker-corrected stereo visual-inertial localisation.

Automation in Construction 156, 105139. DOI: 10.1016/j.autcon.2023.105139.

Wang, P.-H., Wu, R.-B., 2025. An Ultra-Wideband Handover System for GPS-Free Bridge Inspection Using Drones. *Sensors* 25 (6). DOI: 10.3390/s25061923.

Wu, W., Funabora, Y., Doki, S., Doki, K., Yoshikawa, S., Mitsuda, T., Xiang, J., 2024. Evaluation and Enhancement of Resolution-Aware Coverage Path Planning Method for Surface Inspection Using Unmanned Aerial Vehicles. *IEEE Access* 12, 16753–16766. DOI: 10.1109/ACCESS.2024.3359056.